



# The influence of hydrogen on Lomer junctions

Haiyang Yu<sup>a</sup>, Alan C.F. Cocks<sup>b</sup>, Edmund Tarleton<sup>a,\*</sup>

<sup>a</sup> Department of Materials, University of Oxford, Parks Road, Oxford OX1 3PH, UK

<sup>b</sup> Department of Engineering Science, University of Oxford, Parks Road, Oxford OX1 3PJ, UK

## ARTICLE INFO

### Article history:

Received 17 December 2018

Received in revised form 19 February 2019

Accepted 20 March 2019

Available online xxxx

### Keywords:

Hydrogen

Lomer junction

Microcantilever

## ABSTRACT

The influence of hydrogen on Lomer junctions is studied using three dimensional discrete dislocation plasticity simulations which incorporate the hydrogen elastic stress field. Hydrogen can either increase or decrease the junction length, depending on the initial dislocation configuration. However, hydrogen reduces the strength of these junctions, since the Peach-Koehler forces generated by the hydrogen elastic stress field always promote the conversion of a Lomer junction into a Frank-Read source. A microcantilever bend test containing Lomer junctions is simulated showing hydrogen softens the global load-displacement curve, which is partly due to the junction weakening effect revealed here.

© 2019 Acta Materialia Inc. Published by Elsevier Ltd. This is an open access article under the CC BY license (<http://creativecommons.org/licenses/by/4.0/>).

Hydrogen-dislocation interactions are a key aspect of hydrogen embrittlement (HE) and have been investigated extensively [1]. A large amount of experimental evidence suggests that hydrogen facilitates dislocation activity, thereby enhancing localised plasticity [2], which was also supported by theoretical calculations [3], atomistic simulations [4] and dislocation dynamics simulations [5,6]. Recently, a three dimensional hydrogen informed discrete dislocation plasticity (HDDP) model was successfully applied to simulate the influence of hydrogen on dislocation plasticity [6] by implementing analytic expressions for the hydrogen elastic stress field [5] and a hydrogen dependent dislocation mobility law [7].

Three dimensional discrete dislocation plasticity (DDP) considers the interactions of large numbers of dislocation segments belonging to different slip systems, allowing detailed analysis of dislocation junction formation and annihilation [8–10]. If two dislocations, belonging to different slip systems with Burgers vectors  $b_1$  and  $b_2$  intersect and it is energetically favourable,  $b_1^2 + b_2^2 > b_3^2$ , then a dislocation junction can form with Burgers vector  $b_3 = b_1 + b_2$ . Dislocation junctions are often sessile and act as obstacles to dislocation motion and are an important source of work hardening. Hydrogen-junction interaction is key to understanding the influence of hydrogen on plasticity when multiple slip systems are active. However, hydrogen informed DDP simulations to date have focused on single slip and the influence of hydrogen on junctions has not been examined. Chen et al. [11] considered solute-dislocation junction interaction using a coupled kinetic Monte Carlo (kMC)/DDD approach. They performed a parametric study on the influence of solute characteristics, e.g. mobility, size and concentration, based on one initial dislocation configuration. The initial configuration plays an important

role on dislocation junction behaviour [12,13], therefore a systematic investigation of hydrogen solute-junction interactions considering all possible configurations is needed.

In this work, we used a DDP model incorporating the hydrogen elastic stress field [6] to simulate how hydrogen affects the formation and destruction processes of Lomer junctions in face centered cubic (fcc) metals [14]. Hydrogen atoms are approximated as point defects, based on Eshelby's solution [15], in a linear elastic domain in chemical potential equilibrium. Under these assumptions, the hydrogen contribution to the Peach-Koehler (PK) force [5] can be accounted for in the simulation in an efficient manner. For bcc iron, a dislocation mobility law can be estimated as a function of stress and hydrogen concentration [7]. It should also be possible to obtain for Nickel by performing Molecular Dynamics simulation, given the availability of embedded-atom interatomic potentials for hydrogen [16,17]. However, currently a hydrogen dependent dislocation mobility law for Nickel does not exist in the literature. Therefore, we have neglected any influence of hydrogen on dislocation mobility here, i.e. only the hydrogen elastic contribution, also known as the hydrogen shielding effect, was considered. The Lomer junctions formed along [110], the intersection of the (111) and (111) slip planes. Two initial dislocations,  $a/2[101](111)$  (dislocation 1) and  $a/2[011](111)$  (dislocation 2) were considered, where  $a$  is the lattice parameter. Different initial dislocation configurations were simulated by varying  $\phi_1$  and  $\phi_2$  in the range of  $[-\pi, \pi]$ , where  $\phi_1$  ( $\phi_2$ ) is the angle between the line direction of dislocation 1 (dislocation 2) and the line of intersection of the slip planes; the Lomer junction line direction [110], as shown in Fig. 1(a). This is the same geometry used in [13]. A simple linear dislocation mobility law [10] was used, no climb or cross slip was allowed, constraining the motion of glissile dislocations to their glide planes. The Lomer junction was sessile, and its nodes could only move along the line direction. Following [5], the same parameters for Nickel were

\* Corresponding author.

E-mail address: [edmund.tarleton@materials.ox.ac.uk](mailto:edmund.tarleton@materials.ox.ac.uk) (E. Tarleton).

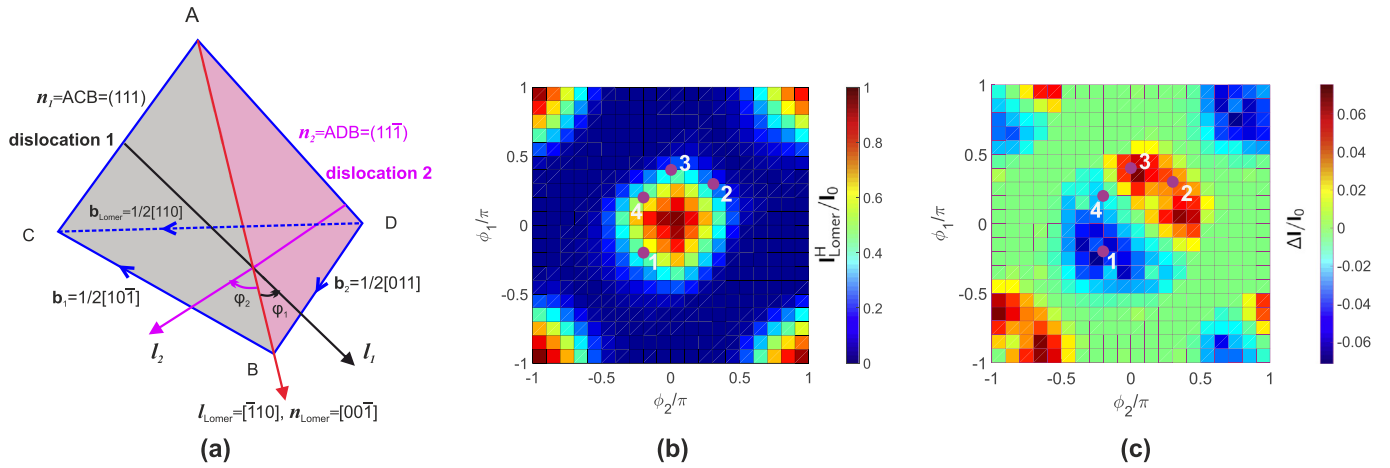


**Fig. 1.** (a) The initial dislocation configuration before relaxation. Dislocation 1 (marked black) is on the (111) plane and has Burgers vector  $\mathbf{b}_1 = \overline{BC} = 1/2[101]$  and line direction  $\mathbf{l}_1$ ; dislocation 2 (magenta) is on the (111) plane and has Burgers vector  $\mathbf{b}_2 = \overline{DB} = 1/2[011]$  and line direction  $\mathbf{l}_2$ . During relaxation, a Lomer junction with  $\mathbf{b}_{\text{Lomer}} = 1/2[110]$  and  $\mathbf{n}_{\text{Lomer}} = [001]$  will be formed along the  $[110]$  direction (red), and the angles of  $\mathbf{l}_1$  and  $\mathbf{l}_2$  with respect to this direction are  $\phi_1$  and  $\phi_2$ , respectively. (b) The contour of normalised Lomer junction length  $l_{\text{Lomer}}^H/l_0$  in  $(\phi_1, \phi_2)$  space, with a hydrogen occupancy of  $\chi_0 = 0.1$ . (c) The hydrogen induced difference in normalised Lomer junction length  $\Delta l/l_0$  in  $(\phi_1, \phi_2)$  space. The four points indicate the four cases selected for the subsequent Lomer junction strength study. (For interpretation of the references to colour in this figure legend, the reader is referred to the web version of this article.)

adopted, and a high initial uniform hydrogen occupancy  $\chi_0 = 0.1$  was applied. Following [11], the cut-off radius for the dislocation stress calculation was  $2b$  and  $b$  for the hydrogen stress calculation. Finally, it should be noted that a steady state hydrogen distribution in equilibrium with the local stress field is assumed throughout this work, which was justified in [18,19]. This approximation is reasonable if  $v\sqrt{\Delta t/D} \ll 1$  [5] which is satisfied if the time increment,  $\Delta t$  is small and at elevated temperatures; as the hydrogen diffusivity,  $D$ , increases rapidly with  $T$  compared to the dislocation mobility  $v$ .

To begin with, the initial dislocation structures were relaxed in the absence of external stress; both dislocations had an initial length of  $l_0 = 400b$ ; the initial angles  $\phi_1$  and  $\phi_2$  were simulated between  $[-\pi, \pi]$  in increments of  $\Delta\phi = \pi/10$ . As discussed by Madec et al. [13], the junction formation is dependent on the initial orientation of the dislocation lines. For some combinations of  $(\phi_1, \phi_2)$ , the dislocations are attracted to each other and form a Lomer junction with a line direction along  $[110]$ ; for other cases, the dislocations repel each other and no junction is formed, in which case the junction length  $l_{\text{Lomer}} = 0$ . Such observations also hold for the case with hydrogen. A surface plot of Lomer junction length in the presence of hydrogen normalised by the initial dislocation length,  $l_{\text{Lomer}}^H/l_0$ , as a function of  $(\phi_1, \phi_2)$  is shown in Fig. 1(b). The junction lengths without hydrogen,  $l_{\text{Lomer}}$  are consistent with those in [13] and so are not repeated here. In both cases, the contour is periodic along  $\phi_1 = \pm \phi_2$  with a wavelength of  $\pi$ . The effect of hydrogen on the Lomer junction length,  $l_{\text{Lomer}}^H$ , can be characterised by  $(l_{\text{Lomer}}^H - l_{\text{Lomer}})/l_0 = \Delta l/l_0$  which is shown in Fig. 1(c). The effect of hydrogen appears small, however, when compared to the values in hydrogen free cases, the relative change in junction length due to hydrogen can be as large as 25% (when  $\phi_1 = \phi_2 = -4\pi/10$ ).

The symmetry and periodicity in the junction length contours allow the effect of hydrogen on Lomer junction strength to be examined for cases which cover the full range. In order to be representative, four cases were selected as indicated on Fig. 1(c): case 1 with  $(\phi_1, \phi_2) = (-2\pi/10, -2\pi/10)$ , case 2 with  $(3\pi/10, 3\pi/10)$ , case 3 with  $(4\pi/10, 0)$ , and case 4 with  $(2\pi/10, -2\pi/10)$ . Case 1 (2) represents the maximum extension (reduction) in the junction length,  $\Delta l$ , along the  $\phi_1 = \phi_2$  line; case 3 represents the maximum hydrogen induced increase in the domain and case 4 is a point on the  $\phi_1 = -\phi_2$  line where the effect of hydrogen is negligible. For these four cases, the initial dislocation lengths were varied from  $l_0 = 200b$  to  $l_0 = 800b$  with an interval of

200b. Relaxation of the dislocation structure without external stress was first simulated, for a sufficiently long time, and Lomer junctions were formed after relaxation in all these cases. A uniaxial tensile stress along  $[100]$  with magnitude  $\sigma$  was then applied to the lock; this is comparable to the stress state in a microcantilever bend test on a single fcc crystal whose  $[100]$  direction is aligned along the longitudinal beam axis.

Under this stress state, the Lomer junction unzips due to the activation of the glissile arms of dislocation 1, while the arms of dislocation 2 remain stationary as the resolved shear stress on slip system 2 is zero. As  $\sigma$  increases the junction length shrinks. When the stress reaches a critical value,  $\sigma_c$ , the Lomer junction length reduces to zero and is annihilated. We define this critical stress as the Lomer junction strength. The junction length with and without hydrogen after relaxation is plotted against the length of the two initial dislocations,  $l_0$ , in Fig. 2(a), and the normalised Lomer junction strength in Fig. 2(b).

Consistent with the observations in Fig. 1, hydrogen can either increase or decrease  $l_{\text{Lomer}}^H$  in Fig. 2(a), depending on the orientation of the two initial dislocations. However in all cases, hydrogen reduces the junction strength,  $\sigma_c$ .

This can be understood by analysing the elastic nodal forces during the evolution of the dislocation structure in the presence of hydrogen. The force on a node  $k$  is partitioned in two parts [6]: the elastic force due to segment-segment interactions and the corrective force due to any applied stresses  $\mathbf{F}_k + \hat{\mathbf{F}}_k$ ; and the force due to the hydrogen elastic shielding effect  $\hat{\mathbf{F}}_k$ , which is scaled  $20\times$  for clarity. Two cases, 1 and 2, are shown in Fig. 3.

The junction formation under relaxation (zipping) and junction annihilation (unzipping) processes for case 1 are illustrated in Fig. 3 (a) and (b). During relaxation the hydrogen generated PK force tends to shorten the Lomer junction. The destruction of the Lomer junction occurs as dislocation 1 expands under the applied tensile stress. The two arms of dislocation 1 (shown in black) are pinned at one end by the junction and at the other end by an initially pinned node. The junction is regarded as sessile, therefore these two line segments are similar to a pair of Frank-Read (F-R) sources, except that one of the pinned nodes is allowed to move along the line direction of the Lomer junction. Once a F-R source is activated, it drives the junction node along the junction line and eventually annihilates the entire Lomer junction. The effect of hydrogen on a F-R source was examined previously [6]. The hydrogen elastic force tends to slow down the motion of pure edge segments and

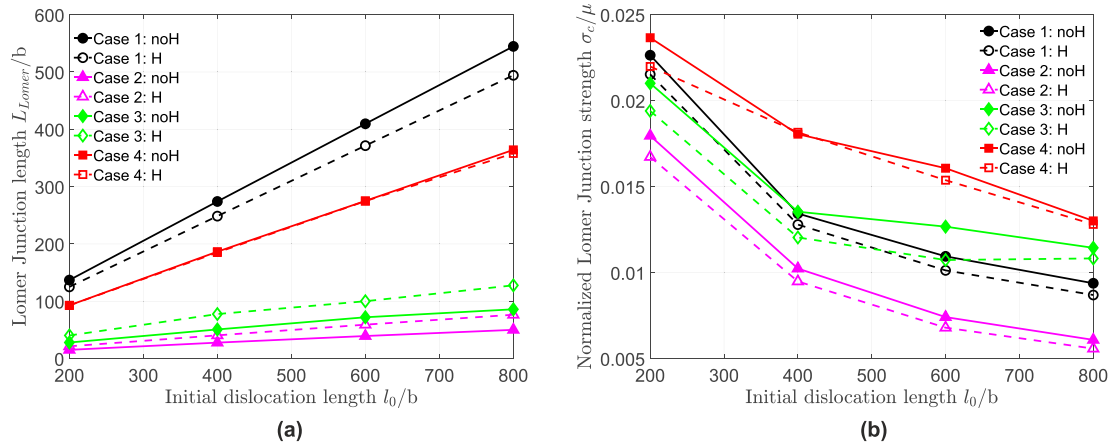


**Fig. 2.** The Lomer junction length and strength versus initial dislocation length for the cases 1–4 with and without hydrogen: (a) the absolute Lomer junction length and (b) the critical uniaxial tensile stress that destroys the Lomer junction, normalised by the shear modulus.

to accelerate the expansion of other parts of the loop, leading to hydrogen enhanced dislocation generation. This is consistent with the observation in Fig. 3(b) where the hydrogen PK forces facilitate the expansion of the half loop and therefore the unzipping process.

In Fig. 3(c), the hydrogen induced PK forces tend to elongate the Lomer junction during its formation. In Fig. 3(d), hydrogen again facilitates the F-R behaviour and the destruction of the junction. These

observations provide a rationale for the curves in Fig. 2. Under relaxation, the hydrogen elastic PK forces can work either collaboratively or in opposition with the segment-segment interaction forces, depending on the initial configuration. Therefore, hydrogen can either lengthen or shorten the Lomer junction. However during the unzipping process, under an applied stress, hydrogen always promotes the expansion of the dislocation half loop promoting the unzipping mechanism in all

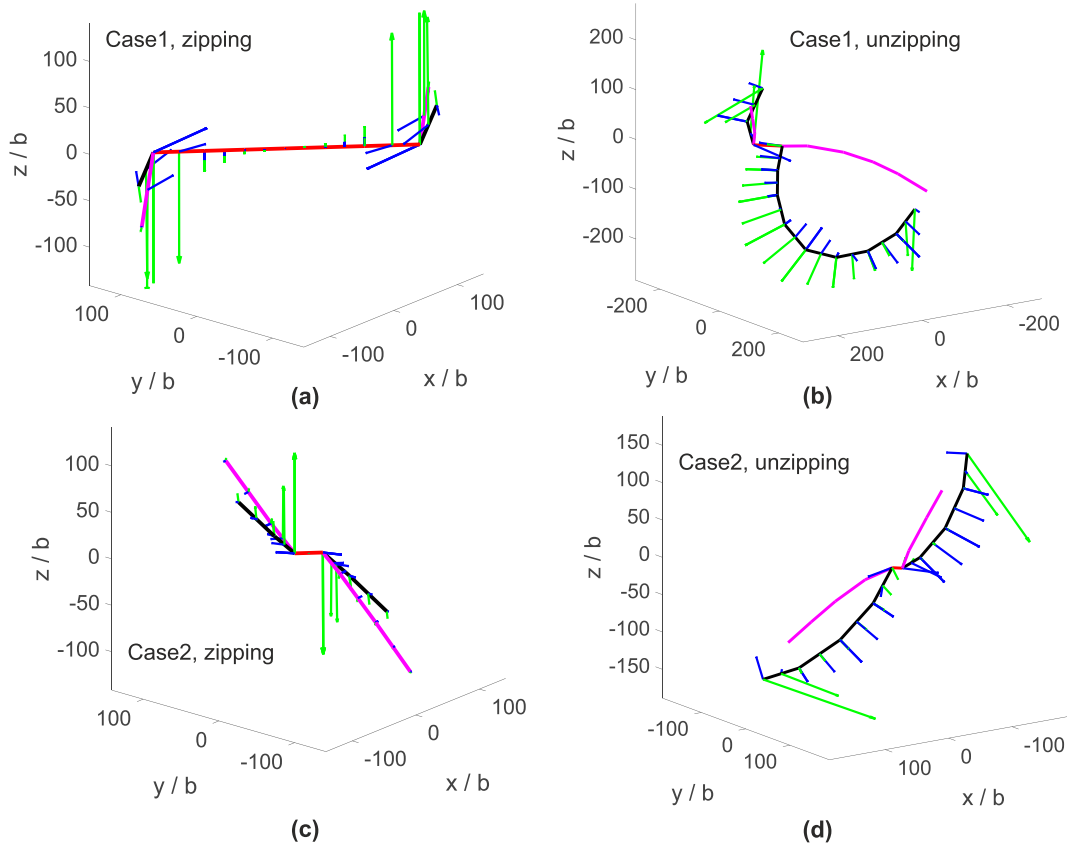


**Fig. 3.** The nodal force partitioned into hydrogen,  $F_k$  (blue arrows), and non-hydrogen parts  $\bar{F}_k + \hat{F}_k$  (green arrows). Showing dislocation 1 (black) and dislocation 2 (magenta) and Lomer junction segments (red). (a) Junction formation during relaxation with no applied stress for case 1. (b) The unzipping process under a uniaxial tensile stress for case 1. (c) Junction formation for case 2 and (d) the unzipping process under uniaxial tension for case 2. The applied tensile stress does not generate a force on dislocation 2, therefore nodal forces are only plotted on dislocation 1 in (b) and (d), and these forces are further projected onto the (111) slip plane. Note  $F_k$  has been scaled  $20\times$  relative to  $\bar{F}_k + \hat{F}_k$  for clarity. The x,y,z axes are aligned along  $[100], [010], [001]$  respectively. (For interpretation of the references to colour in this figure legend, the reader is referred to the web version of this article.)

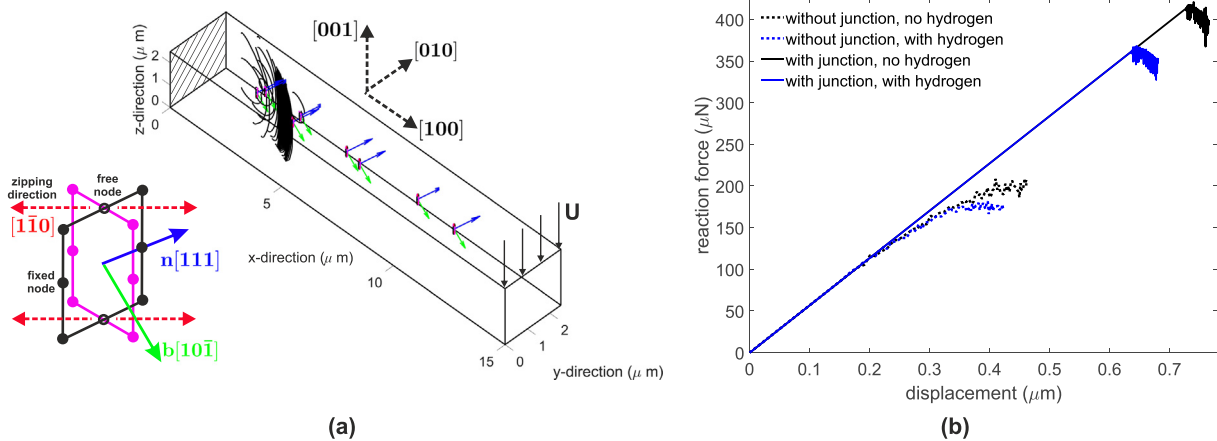


**Fig. 4.** (a) The microcantilever simulation with randomly distributed sources. Each source consists of two intersecting prismatic loops. The black (magenta) loop has the same slip system as dislocation 1 (2) in Fig. 1(a). The plane normal  $\mathbf{n}$  and the Burgers vector  $\mathbf{b}$  for dislocation 1 are plotted while those for dislocation 2 are omitted for clarity. Except for the two intersecting nodes, the other initial nodes are fixed. (b) The hydrogen and hydrogen free load-displacement curves with initial prismatic loop sources and Lomer junctions. (For interpretation of the references to colour in this figure legend, the reader is referred to the web version of this article.)

cases. In other words, hydrogen always weakens Lomer junctions. A similar process occurs in cases 3 and 4 and is therefore not repeated. It should be noted that the Lomer strength also depends on the junction length,  $\sigma_c \sim \mu b / (l_0 - l_{Lomer}^H)$ , and the junction length is hydrogen dependent [11]. If the Lomer junction length is increased due to hydrogen, the arm length left on dislocation 1 will be decreased; this gives a shorter F-R source which is harder to activate, hence an increased junction strength. However, this effect is negligible compared to the tendency of the hydrogen forces to facilitate dislocation loop expansion, as indicated by cases 2 and 3 in Fig. 2.

Hydrogen can soften the mechanical response by enhancing the operation of F-R sources [6]. By weakening Lomer junctions hydrogen is predicted to further promote dislocation plasticity. To verify this assumption, end-loaded microcantilever bend tests were simulated. The beam was fixed at one end with a displacement applied at the other. Pairs of intersecting prismatic loops were randomly distributed inside the volume, as shown in Fig. 4(a). These loops were first allowed to relax and form Lomer junctions along the zipping direction [110]. Upon bending an approximately uniaxial stress is generated which is tensile (or compressive) on the Lomer junction located above (or below) the neutral plane. This causes the junctions to unzip as the applied load increases, as shown in Fig. 3; dislocation 2 (magenta) remained stationary as the resolved stress was zero, while dislocation 1 (black) bowed out and operated as a F-R source. Therefore dislocation nucleation requires a junction conversion into a F-R source followed by the usual F-R source operation. Simulations were also performed with prismatic loop sources all belonging to the same  $1/2[101](111)$  slip system (black loops in the figure) and each loop can act as a pair of F-R sources. Lomer junction and prismatic loop sources were simulated with and without hydrogen. These simulations are idealised and a statistical approach is needed to fully quantify the effect of hydrogen on plasticity. Here we focus on how junction weakening by hydrogen influences the mechanical response. We continue to assume equilibrium of chemical potential (fast diffusion); this assumption is appropriate as long as the loading rate is sufficiently low [19]. In general the results obtained under the fast diffusion assumption are a useful upper bound on the influence of hydrogen.

The load-displacement curves are plotted in Fig. 4(b). With Lomer sources the onset of plasticity is delayed, compared to the simulations with prismatic loop sources, due to the stress needed to convert the Lomer junctions into F-R sources. Hydrogen weakens Lomer junctions, promoting their conversion to F-R sources and then promotes the operation of F-R sources. In the simulations without junctions, hydrogen

only enhances F-R operation. In both cases, yielding occurs earlier in the presence of hydrogen, as expected. Further, it is observed that hydrogen causes a more pronounced and sudden drop in the case with junctions. Indicating that the hydrogen weakening junction mechanism revealed in this work plays an important role in hydrogen enhanced plasticity. In reality, F-R sources and junctions should be included in the initial structure then the response is expected to be between the limits in Fig. 4(b).

In summary, the influence of hydrogen on the zipping and unzipping of Lomer junctions was simulated. Hydrogen could either promote or impede the junction formation in the absence of an external stress, depending on the initial dislocation configuration. However, hydrogen facilitated the destruction of these junctions in all the cases investigated, in other words, hydrogen always weakens Lomer junctions. This is because the hydrogen elastic force acts to bow out the dislocation segments at either end of the junction to form Frank-Read sources which then annihilate the junction. Therefore hydrogen acts to convert the Lomer junction into a F-R source. Then once operating, hydrogen acts to enhance the nucleation of loops from a F-R source as shown in [6]. Hydrogen weakening of Lomer junctions is likely a contributor to hydrogen enhanced plasticity, as verified by a simple microcantilever bend test.

It should be noted that only hydrogen elastic shielding was considered here, and the influence of hydrogen on the core force or dislocation mobility was neglected. A very large initial bulk hydrogen concentration was considered here to illustrate the effect of hydrogen elastic shielding on Lomer junctions. The effect at lower, more realistic, hydrogen concentrations is less pronounced. To model the full effect of hydrogen on dislocation junctions at a realistic bulk concentration, will require a hydrogen dependent core force to be quantified and implemented within DDP. This is in progress, it is expected that the current conclusions will not be changed qualitatively when the hydrogen core force is included.

## Acknowledgements

This work was supported by the Engineering and Physical Sciences Research Council under Programme grant EP/L014742/1 and Fellowship grant EP/N007239/1.

## Appendix A. Supplementary data

Supplementary data to this article can be found online at <https://doi.org/10.1016/j.scriptamat.2019.03.022>.

## References

- [1] I.M. Robertson, P. Sofronis, A. Nagao, M.L. Martin, S. Wang, D.W. Gross, K.E. Nygren, *Metall. Mater. Trans. B Process Metall. Mater. Process. Sci.* 46 (2015) 1085–1103.
- [2] I.M. Robertson, *Eng. Fract. Mech.* 68 (2001) 671–692.
- [3] H.K. Birnbaum, P. Sofronis, *Mater. Sci. Eng. A* 176 (1994) 191–202.
- [4] M. Itakura, H. Kaburaki, M. Yamaguchi, T. Okita, *Acta Mater.* 61 (2013) 6857–6867.
- [5] Y. Gu, J.A. El-Awady, *J. Mech. Phys. Solids* 112 (2018) 491–507.
- [6] H. Yu, A.C.F. Cocks, E. Tarleton, *J. Mech. Phys. Solids* 123 (2019) 41–60.
- [7] I.H. Katzarov, D.L. Pashov, A.T. Paxton, *Phys. Rev. Mater.* 1 (2017), 033602.
- [8] H.M. Zbib, M. Rhee, J.P. Hirth, *Int. J. Mech. Sci.* 40 (1998) 113–127.
- [9] V.B. Shenoy, R.V. Kukta, R. Phillips, *Phys. Rev. Lett.* 84 (2000) 1491–1494.
- [10] S.W. Lee, S. Aubry, W.D. Nix, W. Cai, *Model. Simul. Mater. Sci. Eng.* 19 (2011), 025002.
- [11] Q. Chen, X.Y. Liu, S.B. Biner, *Acta Mater.* 56 (2008) 2937–2947.
- [12] D. Rodney, R. Phillips, *Phys. Rev. Lett.* 82 (1999) 1704.
- [13] R. Madec, B. Devincere, L.P. Kubin, *Phys. Rev. Lett.* 89 (2002), 255508.
- [14] D. Hull, D.J. Bacon, *Introduction to Dislocations*, fifth ed. Butterworth-Heinemann, Oxford, 2011.
- [15] J.D. Eshelby, *Acta Metall.* 3 (1955) 487–490.
- [16] M.S. Daw, M.I. Baskes, C.L. Bisson, W.G. Wolfer, Modeling environmental effects on crack growth processes: Proceedings of a Symposium, in: R.H. Jones, W.W. Gerberich (Eds.), TMS-AIME, New York 1986, pp. 99–124.
- [17] M. Ruda, D. Farkas, J. Abriata, *Phys. Rev. B* 54 (1996) 9765–9774.
- [18] D. Delafosse, 9 - hydrogen effects on the plasticity of face centred cubic (fcc) crystals, in: R.P. Gangloff, B.P. Somerday (Eds.), *Gaseous Hydrogen Embrittlement of Materials in Energy Technologies*, Elsevier, Cambridge 2012, pp. 247–285.
- [19] R.B. Sills, W. Cai, *Philos. Mag.* 98 (2018) 1491–1510.